

## Hemispheric dispersion of radioactive plume laced with fission nuclides from the Fukushima nuclear event

Shih-Chieh Hsu,<sup>1</sup> Chih-An Huh,<sup>2</sup> Chuen-Yu Chan,<sup>3</sup> Shuen-Hsin Lin,<sup>1</sup> Fei-Jan Lin,<sup>4</sup> and Shaw Chen Liu<sup>1</sup>

Received 12 October 2011; revised 30 November 2011; accepted 9 December 2011; published 12 January 2012.

[1] Radioactivities of particulate  $^{131}\text{I}$  and  $^{137}\text{Cs}$  released from the Fukushima nuclear accident were monitored in a regional aerosol network including two high mountain sites (central Taiwan and Tibetan Plateau). The results were integrated with data measured elsewhere around the world, with special focus on the mid-latitudes. The hemispheric transport of the Fukushima radiation clouds (FRCs) by the westerlies took  $\sim 18$  days, displaying an exponential-like decrease eastward, with a dilution factor of at least five orders of magnitude following a full circuit around the globe. The initial two waves of FRCs may travel at different altitudes: the first one at  $\sim 3\text{--}4$  km, whereas the second one up to 5 km or more.  $^{131}\text{I}$  and  $^{137}\text{Cs}$  were fractionated during transport, with  $^{137}\text{Cs}$  concentrated in the shallower layer, susceptible to depositional removal, while  $^{131}\text{I}$  moving faster and higher. This accident may be exemplified to identify some atmospheric processes on the hemispheric scale. **Citation:** Hsu, S.-C., C.-A. Huh, C.-Y. Chan, S.-H. Lin, F.-J. Lin, and S. C. Liu (2012), Hemispheric dispersion of radioactive plume laced with fission nuclides from the Fukushima nuclear event, *Geophys. Res. Lett.*, 39, L00G22, doi:10.1029/2011GL049986.

### 1. Introduction

[2] The 2011 Tohoku-Oki Earthquake, also known as the Great East Japan Earthquake, with a magnitude of 9.0 ( $M_w$ ), took place at 14:46 JST (05:46 UTC) on 11 March 2011 off the eastern coast of Japan. It is believed to be the most powerful earthquake to have struck Japan ([http://en.wikipedia.org/wiki/2011\\_T%C5%8Dhoku\\_earthquake\\_and\\_tsunami](http://en.wikipedia.org/wiki/2011_T%C5%8Dhoku_earthquake_and_tsunami)). An extremely destructive tsunami followed the earthquake and produced waves of  $>30$  m high [Fujii *et al.*, 2011]. As a consequence, the dual natural disaster instantaneously inundated nearby Japanese coastal villages, along with the Fukushima I (Daiichi) Nuclear Power Plant ( $37^{\circ}25'17''\text{N}$ ,  $141^{\circ}1'57''\text{E}$ ), causing a nuclear accident that put the whole world on alert. Three of the six reactors at the power plant experienced meltdowns (or even melt-throughs) a few hours to a few days after the cataclysmic disaster. This fact has been declared by the Tokyo Electric Power Company (TEPCO) on 23 May 2011 [Tokyo Electric Power Company, 2011]. The disaster at the power plant resulted in massive

releases of radioactive materials into the local air, ocean, soil, ground water, and so on [Normile, 2011; Morino *et al.*, 2011; Stohl *et al.*, 2011]. Through the atmosphere, Fukushima radiation clouds (FRCs) quickly spread around the globe. In the U.S., elevated  $^{133}\text{Xe}$  (half life  $T_{1/2} = 5.2$  d), up to  $40$  Bq/m<sup>3</sup> and four orders of magnitude higher than the average background concentration were detected at the Pacific Northwest National Laboratory (PNNL;  $46^{\circ}16'47''\text{N}$ ,  $119^{\circ}16'53''\text{W}$ ) early on 16 March [Bowyer *et al.*, 2011]. The global model simulation has shown that radioactive substances emitted from the Fukushima Daiichi Nuclear Power Plant have been transported over the North Hemisphere. However, the simulation results emphasized its influence on the North America and poleward dispersion over Euro-Asia, and there were little observation data for verification [Takemura *et al.*, 2011].

[3] We present observation data on particulate  $^{131}\text{I}$  ( $T_{1/2} = 8.02$  d),  $^{137}\text{Cs}$  ( $T_{1/2} = 30.1$  y), and  $^{134}\text{Cs}$  ( $T_{1/2} = 2.06$  y) gathered from a Tibetan Plateau station (Nam Co, 4700 m) and compile these together with our recently published data gathered from another high mountain station (Mt. Lulin, central Taiwan; 2782 m), two offshore island stations (one in the East China Sea and another in the South China Sea), and one station in north Taiwan [Huh *et al.*, 2012]. We collate additional reported data from sources around the world, particularly the CTBTO (Comprehensive Nuclear-Test Ban Treaty Organization) observation network [Masson *et al.*, 2011]. We then discuss the hemispheric transport of Fukushima-derived radionuclides, with an emphasis on the Earth's northern middle latitudes. Finally, we construct a schematic model for explaining the hemispheric dispersion.

### 2. Materials and Methods

[4] After the Fukushima Daiichi Nuclear Power Plant accident on March 11, fission nuclides  $^{131}\text{I}$  (hereafter representing particulate  $^{131}\text{I}$  unless specifically indicating gaseous fraction or all phases),  $^{137}\text{Cs}$ , and  $^{134}\text{Cs}$  in particulate form were measured continuously till early May through aerosol filter samples collected over a sampling network, which includes two offshore-island ground-level stations (Pengchiayu in the East China Sea, and Dongsha in the South China Sea, denoted as PCY and DS, respectively) ( $25^{\circ}37'12''\text{N}$ ,  $122^{\circ}4'12''\text{E}$ ;  $20^{\circ}41'54''\text{N}$ ,  $116^{\circ}43'43''\text{E}$ ) and two Taiwan inland stations (Nankang at ground level in northern Taiwan and Mt. Lulin at 2862 m high in central Taiwan, denoted as NK and MLL, respectively) ( $25^{\circ}2'26''\text{N}$ ,  $121^{\circ}36'50''\text{E}$ ;  $23^{\circ}28'07''\text{N}$ ,  $120^{\circ}52'25''\text{E}$ ) (Figure 1). During the sampling period and over the sampling area, the layer of  $\sim 1.5$  km high is under the influencing regime of the prevailing northeasterly monsoon. In contrast, the westerlies were the prevailing winds at the elevation of MLL. Sampling

<sup>1</sup>Research Center for Environmental Changes, Academia Sinica, Taipei, Taiwan.

<sup>2</sup>Institute of Earth Sciences, Academia Sinica, Taipei, Taiwan.

<sup>3</sup>School of Environmental Science and Engineering, Sun Yat-Sen University, Guangzhou, China.

<sup>4</sup>Institute of Oceanography, National Taiwan University, Taipei, Taiwan.

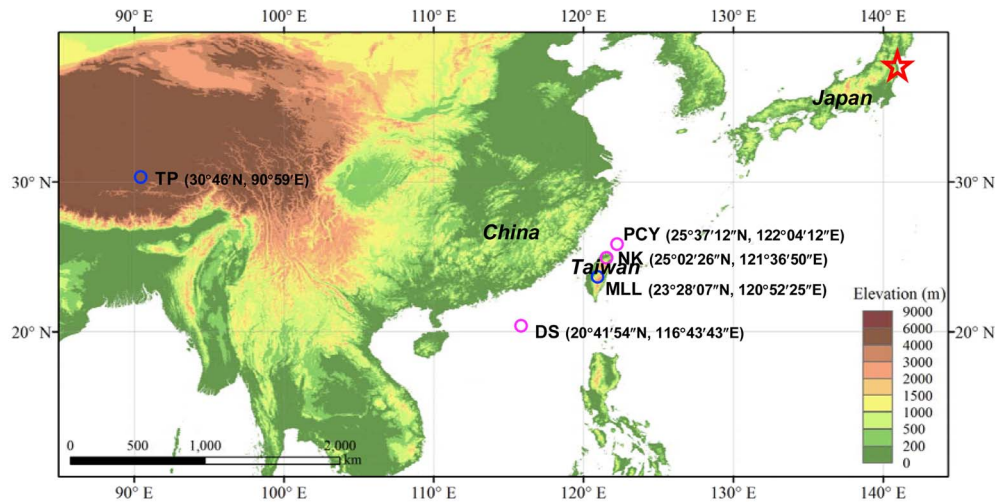


**Figure 1.** A regional total suspended particle (TSP) sampling network, including three ground level stations (indicated by pink circles), namely, Pengchiayu (PCY), Dongsha (DS), and Nankang (NK) in northern Taiwan, and two high mountain stations (blue circles), namely, Mt. Lulin (MLL; 2862 m) in central Taiwan, and Nam Co (4730 m) on the Tibetan Plateau (TP).

was terminated at DS on March 31 because of sampler malfunctions. The sampling was also suspended at NK from April 2 to April 5 due to shortage of hands at such a crunch time. These interruptions, however, do not affect our interpretation of the time series as the signals of first arrival have been caught and the temporal trends at PCY and NK are largely analogous (Figure 2), as will be described later. In general, the sampling was conducted with a daily sampling frequency for most samples and a bi-daily frequency for a few NK samples. In addition, the filter samples were collected at the Nam Co station ( $30^{\circ}46'N$ ,  $90^{\circ}59'E$ ; 4730 m) on the Tibetan Plateau (denoted as the TP station) from 15 March to 6 April with a

5–6 day sampling frequency. This station is, expectedly, under the sway of stronger westerly jet streams.

[5] The aerosol samples were collected through a 24-hour pumping of  $\sim 1700 \text{ m}^3$  air through cellulose filters ( $8'' \times 10''$  in size) by a high-volume TSP sampler (TE-5170D), which generally can collect particles larger than  $0.03 \mu\text{m}$  [Hsu *et al.*, 2010, and references therein]. Five HPGc detectors with 100%–150% efficiency (relative to  $3 \times 3 \text{ NaI}$ ) were used to provide the necessary throughput for the efficient counting of the daily samples returned from all observation sites. The activities of  $^{131}\text{I}$ ,  $^{134}\text{Cs}$ , and  $^{137}\text{Cs}$  in each sample were calculated based on the counts registered under the

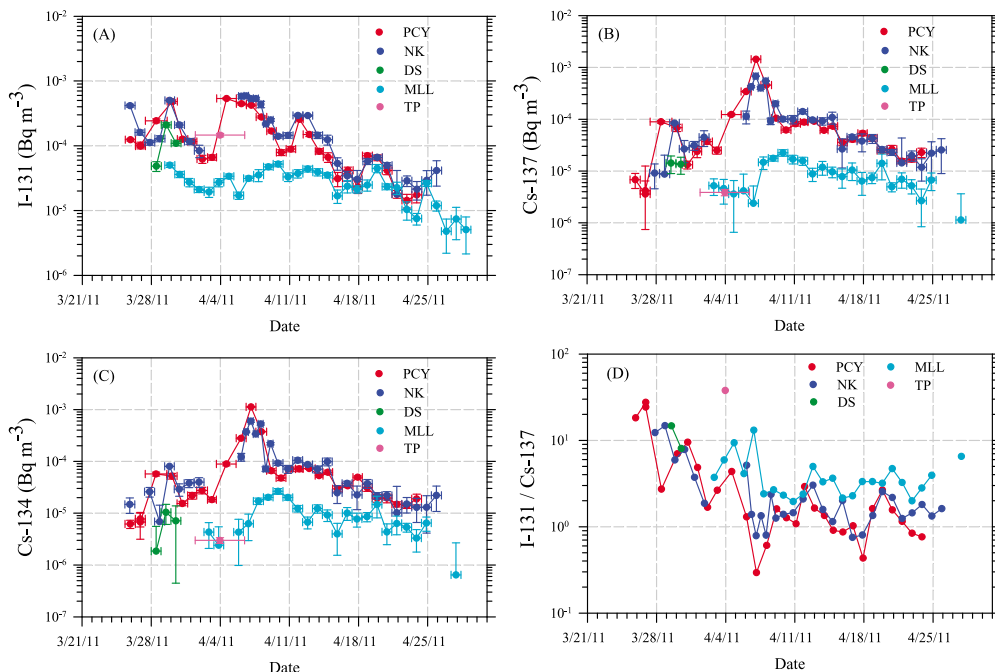


**Figure 2.** Time-series of (a)  $^{131}\text{I}$ , (b)  $^{137}\text{Cs}$ , and (c)  $^{134}\text{Cs}$  activities, and (d) the  $^{131}\text{I}/^{137}\text{Cs}$  activity ratio at the five observation stations, namely, PCY, NK, DS, MLL, and TP. The data for the former four stations have been reported by Huh *et al.* [2012]. Data below detection limits are not shown in the plots although samples collected before the arrival time at each site have been analyzed. The overall dataset can be found in Data Set S1 in the auxiliary material.

photon peaks centered at 364.48 keV, 604.66 keV, and 661.62 keV, respectively. Detailed description about sampling and analyses is given in the auxiliary material.<sup>1</sup> Data reported here (Data Set S1) were from the dates (since 25 March) when the Fukushima signal was first detected to the dates (in late April 2011) when the target nuclides cannot be detected (i.e., below detection limits).

### 3. Results and Discussion

#### 3.1. Time-Series of <sup>131</sup>I, <sup>137</sup>Cs, <sup>134</sup>Cs, and the <sup>131</sup>I/<sup>137</sup>Cs Activity Ratio

[6] Overall, the activities of the three radionuclides analyzed were considerably low, almost all of which registered below  $10^{-3}$  Bq/m<sup>3</sup>, with the exception of <sup>137</sup>Cs and <sup>134</sup>Cs at PCY during April 6–7. The amounts of radionuclides were far lower than the amounts detected anywhere from Japan, across north America and Europe and therefore posed little risk in terms of public health concerns. In addition, the radionuclides were around one order of magnitude lower at MLL compared with those at PCY and NK. As shown in Figure 2a, the time-series of <sup>131</sup>I activity shows that <sup>131</sup>I was detected at ground stations PCY and NK since 25 March, and at DS since 27 March. At least two relatively significant waves of radiation clouds appeared at PCY and NK as there were two concentration maxima measured around March 29 and April 5. Sharp declines in the activity of <sup>131</sup>I, <sup>137</sup>Cs and <sup>134</sup>Cs began since mid-April. <sup>131</sup>I was not detected at MLL until 29 March and not detected at TP until April (i.e., in the sample collected during April 1–6), significantly later than at MLL.

[7] Since <sup>137</sup>Cs and <sup>134</sup>Cs were closely coupled and presented a similar time-series at each station (Figures 2b and 2c), only <sup>137</sup>Cs is discussed hereafter. In general, <sup>137</sup>Cs exhibited a similar time-series with <sup>131</sup>I at the three ground stations. However, <sup>137</sup>Cs presented very low activities in the first wave and arrived late in the second wave relative to <sup>131</sup>I particularly at PCY. Based on our daily resolution, the decoupled peaks of <sup>131</sup>I and <sup>137</sup>Cs at PCY seem to be coupled together while arriving at NK in the Taipei Basin. Meanwhile, <sup>137</sup>Cs was still not detectable at MLL until four days after <sup>131</sup>I was detected, i.e., on April 2. The coupling or the decoupling of <sup>131</sup>I and <sup>137</sup>Cs may result in variable <sup>131</sup>I/<sup>137</sup>Cs ratios, as depicted in Figure 2d. These may indicate either distinctive radionuclide leakage stages respondent to the state of the damaged nuclear reactors, or differentiation of the two kinds of radionuclides (iodine and cesium) during transport, which are discussed later.

#### 3.2. Compilation of Data Reported at the Mid-latitudes of the North Hemisphere

[8] To understand a full picture of hemispheric transport and the resulting evolution of the FRCs, we further compile additional data from all over the world on the monitored radionuclides, from the source (Japan) eastward to the downwind receiving regions, including our stations TP and MLL, with particular focus on the mid-latitudes under the influence of the westerly winds, including Takasaki (denoted as TA; 36.3°N, 139.1°E), Japan; the west coast of the US (University of

California, Berkeley campus, denoted as UCB; 37.87°N, 122.26°W) and the east coast of the US (Charlottesville, VA, denoted as USP75; 38.0°N, 78.4°W); Greece (40.63°N, 22.97°E), southeastern Europe; TP and MLL. Among these sites, TA and USP75 stations (RN38 and RN75) are under the CTBTO worldwide radionuclide monitoring network (<http://www.ctbto.org/press-centre/highlights/2011/fukushima-related-measurements-by-the-ctbto/fukushima-related-measurements-by-the-ctbto-page-1/>). The UCB data can be verified from the website of the Department of Nuclear Engineering, UC Berkeley (<http://www.nuc.berkeley.edu/UCBAir-Sampling/AirSamplingResults>). The data from Greece were published by *Manolopoulou et al.* [2011]. Since <sup>131</sup>I was detected at TA on March 15, there were two spiking concentrations. The first spike appeared on the first day when <sup>131</sup>I was detected, whereas the second one appeared five days later (March 20). Therefore, only the data detected within the initial ~10 days (i.e., the period covering the complete first two waves of the FRCs) were considered in this study to illustrate the hemispheric transport. At UCB, USP75, and in Greece, <sup>131</sup>I was first detected on March 18, 19, and 24, respectively. According to the report of the Ministry of Environmental Protection (MEP) in China ([http://big5.mep.gov.cn/gate/big5/www.mep.gov.cn/zhxx/xwfb/index\\_2.htm](http://big5.mep.gov.cn/gate/big5/www.mep.gov.cn/zhxx/xwfb/index_2.htm)), <sup>131</sup>I was detected extensively over China from March 27 to 30. Overall, the timing of the arrivals of the radionuclides coincided with one another, with the exception of TP. According to the report by the MEP of China that the Tibet autonomous region was the last area over China that detected the FRCs ([http://big5.mep.gov.cn/gate/big5/www.mep.gov.cn/zhxx/xwfb/index\\_2.htm](http://big5.mep.gov.cn/gate/big5/www.mep.gov.cn/zhxx/xwfb/index_2.htm)); the arrival time of the radiation cloud on the Tibetan Plateau was exactly determined on April 2, even later than at MLL. This means that either the first wave of the FRCs did not pass TP or that it was transported below the altitude of the station.

[9] Figure 3 shows that, <sup>131</sup>I and <sup>137</sup>Cs decreased downwind exponentially with an increase in travel distance and, possibly, time. The decreasing trend conceivably results from a complex process involving dispersion, sedimentation and decay. Decay for <sup>137</sup>Cs could be ignored as its half-life (30 years) is much longer than the time scale of this special event. Although the decay of the short-lived <sup>131</sup>I is quite significant in its global journey, it is still a less important factor in reducing radioactivities when compared with the effect of diffusion and mixing [*Priyadarshi et al.*, 2011]. Nevertheless, we still performed decay correction for the time elapsed from 12 March 2011 to the first arrival time of <sup>131</sup>I at each site, which were 0.5, 6, 7.5, 12, 14 and 18 days at TA, UCB, USP75, Greece, TP and MLL, respectively. These plots demonstrate that the dilution factor of the Fukushima radiation after the hemispheric dispersion may be around five orders of magnitude for each of <sup>131</sup>I and <sup>137</sup>Cs as their activity concentrations decreased from  $10^0$  and  $10^{-1}$  Bq/m<sup>3</sup>, respectively, at TA to  $10^{-5}$  and  $10^{-6}$  Bq/m<sup>3</sup>, respectively, at MLL. However, we noted that TA is located ~210 km southwest of the Fukushima Nuclear Power Plant, likely resulting in relatively low radioactivities compared with the levels found in the eastern coastal sides, where official quality data are unavailable. Hence, it might be unable to adequately represent the initial emissions of radionuclides. This would further result in a dilution factor larger than those expected in this study.

<sup>1</sup>Auxiliary material data sets are available at <ftp://ftp.agu.org/apend/gl/2011gl049986>.

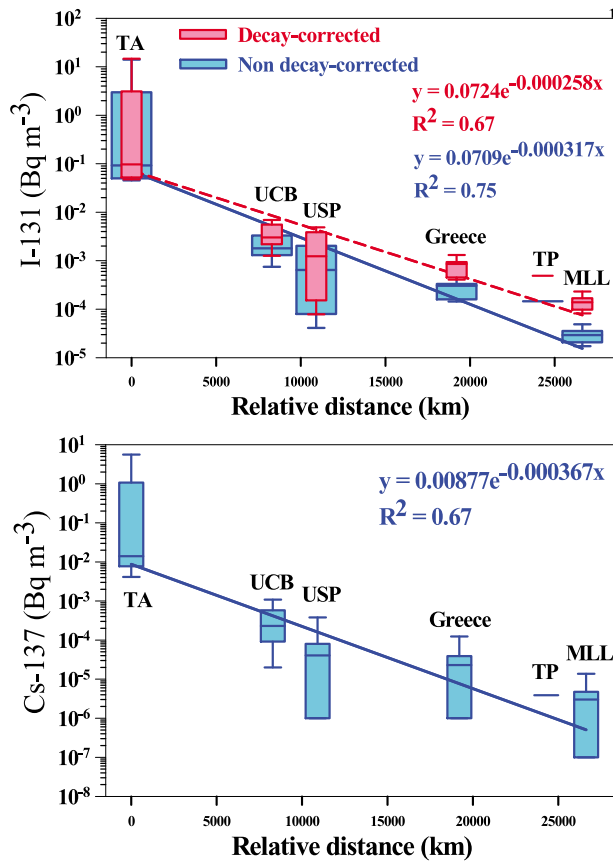


**Figure 3.** Exponential-like decreasing trends of (top)  $^{131}\text{I}$  and (bottom)  $^{137}\text{Cs}$  activities in mid-latitude regions of the North Hemisphere. TP is excluded from the regression analysis (see text for explanation). Data used here basically were taken from a  $\sim 10$ -day period essentially covering the initial two waves of the FRCs, except TP (5 days): 15–24 March for TA; 19–27 March for UCB; 19–28 March for USP 75; 24 March–5 April for Greece; 1–6 April for TP; and 29 March–7 April for MLL. For  $^{131}\text{I}$ , decay effect was considered and data with decay-based correction are thus shown along with the raw (non decay-corrected) data. In each plot, the ends of the box, the ends of the whiskers, and the line across each box represent the 25th and 75th percentiles, the 5th and 95th percentiles, and the median, respectively.

[10] Because of two reasons, TP is excluded from the regression. First, the first wave of FRCs might not reach this site. Second, the elevation of this site is much higher than other sites and thus it is irrelevant to compare with other sites. The equations for the regression lines are  $y = 0.0724 e^{-0.000317x}$  for non-decay corrected  $^{131}\text{I}$ , with  $R^2 = 0.67$ , and  $y = 0.00877 e^{-0.000367x}$  for  $^{137}\text{Cs}$ , with  $R^2 = 0.67$ . While the leading coefficients of the two equations (i.e., 0.0724 versus 0.00877) are rather different, the exponents (i.e.,  $-0.000317$  versus  $-0.000367$ ) are fairly close. The former reflects different magnitudes of  $^{131}\text{I}$  and  $^{137}\text{Cs}$  activities released from the Fukushima source, and the latter represents rates of decrease of radioactivity due to mixing, decay and sedimentation during the hemispheric transport. Sedimentation might be less effective in removing  $^{131}\text{I}$  which is mostly associated with very fine particles with diameters of around  $0.4 \mu\text{m}$  [Jost et al., 1986]. This may lead to a longer

suspension for  $^{131}\text{I}$ -laden aerosol. Cs-137 is characterized by its particle-reactive nature and is mainly associated with  $\sim 1 \mu\text{m}$  sized particles [Jost et al., 1986], presumably resulting in relatively rapid sedimentation out of the atmosphere, as reflected in the more negative exponent (i.e.,  $-0.000367$ ) for the regression line of  $^{137}\text{Cs}$ . On the other hand, total  $^{131}\text{I}$  in the initial emission existed predominantly ( $\sim 90\%$ ) in the gaseous form [Morino et al., 2011], which would be gradually attached onto tiny aerosol particles while traveling. Longer suspension of submicron-sized aerosol particles may partly offset the decay of  $^{131}\text{I}$  during transport. The USA's EPA (<http://www.epa.gov/radiation/rert/radnet-kauai-exprate.html#air>) collected samples in Kauai, Hawaii on March 21 and 22 using both the air cartridge and the air filter sampling techniques, of which the former can collect  $^{131}\text{I}$  in both gaseous and particulate phases (i.e., the total  $^{131}\text{I}$ ) while the latter can collect only the particulate phase. The measured activity concentrations of  $^{131}\text{I}$  on March 21 and March 22 were respectively 1.07 and 0.18  $\text{Bq}/\text{m}^3$  using the cartridge samples versus 0.39–0.52 and 0.07–0.089  $\text{Bq}/\text{m}^3$  using the filter samples. This demonstrates that gaseous  $^{131}\text{I}$  is gradually adsorbed onto aerosol particles in the downwind region, resulting in  $\sim 50\%$  of the total  $^{131}\text{I}$  in the particulate form around Hawaii. In the farther downwind region, the particulate phase may further increase and become predominant, exceeding the gaseous phase; this suggestion is, however, at odds with Masson et al. [2011].

### 3.3. Hemispheric Transport of Fukushima Derived Radioactive Nuclides

[11] The journey of the FRCs around the globe took  $\sim 18$  days. This is much longer than the time ( $\sim 10$  days) it took for the radiation clouds emitted from the Chernobyl disaster to do the same [Harrison et al., 1993], and it is still longer than the time ( $\sim 13$  days) for Asian dust to go around the world [Uno et al., 2009]. However, the FRCs took a slightly shorter time than the time ( $\sim 22$  days) for the  $\text{SO}_2$  plumes emitted by the Mount Pinatubo Eruption to go around the world [Bluth et al., 1992]. Apparently, the speed of travel depends on the location (particularly latitudes) of the source of emission and the vertical height that the emission can ascend to, along with the synoptic weather and the atmospheric conditions. Judging from the arrival times of  $^{131}\text{I}$  at TP and MLL, it's possible that the first wave of FRCs was confined within a shallower layer of less than  $\sim 3$ – $4$  km and thus not detected at TP, whereas the second wave may have reached 5 km or higher. Also, this observation can be attributed to mechanical problems in the distinct stages of the power plant reactor cores' meltdown, as observed in the Chernobyl Event, during which the radiation plumes reached a  $\sim 2$  km elevation in the initial explosion [Brandt et al., 2002] and were subsequently entrained to the upper troposphere or higher [Pudykiewicz, 1989].

[12] The CTBTO Preparatory Commission reported the detection of two waves of  $^{131}\text{I}$  radiation clouds during the initial ten days (3/15–3/24) at TA, with  $^{131}\text{I}$  activities up to 15 and 5.3  $\text{Bq}/\text{m}^3$  on March 15 and 20, whereas the corresponding  $^{137}\text{Cs}$  activities were 5.8 and 3.7  $\text{Bq}/\text{m}^3$  on the same two days. The resultant  $^{131}\text{I}/^{137}\text{Cs}$  ratios were as low as 2.6 and 1.4. In early June, the Japanese government and TEPCO admitted that the core of Reactor 1 experienced a meltdown (or even a melt-through) 5 hours after the catastrophic earthquake [Tokyo Electric Power Company, 2011].

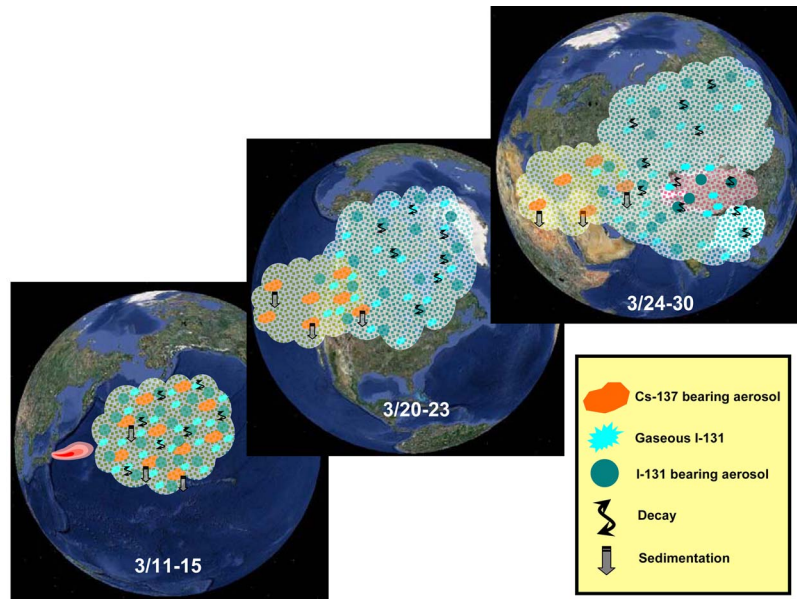


**Figure 4.** The schematic of a conceptual model for the hemispheric transport of Fukushima-derived radiation clouds, focusing at the mid-latitudes.

Reactors 2 and 3 may also have suffered from a meltdown in the ensuing days. This may explain the concurrence of elevated  $^{131}\text{I}$  and  $^{137}\text{Cs}$  and the low  $^{131}\text{I}/^{137}\text{Cs}$  ratio at TA. However, the activities of  $^{137}\text{Cs}$  measured at the downwind mid-latitude stations were mostly very low, even below the detection limits, in the early days when  $^{131}\text{I}$  arrived, leading to elevated  $^{131}\text{I}/^{137}\text{Cs}$  ratios. For example,  $^{137}\text{Cs}$  was not detected at the MLL station until April 2, a much later date than the first detection of  $^{131}\text{I}$ . The same scenario was reported at the USP75 and the Greece stations [Manolopoulou *et al.*, 2011]. Similarly,  $^{137}\text{Cs}$  was very low in our April 1–6 TP sample, with a resulting  $^{131}\text{I}/^{137}\text{Cs}$  ratio of 38. According to the monitoring results of the MEP of China,  $^{137}\text{Cs}$  had never been detected on the TP (i.e., below the detection limit). This contrasts with the results at TA.

[13] We have observed a decoupling of  $^{131}\text{I}$  and  $^{137}\text{Cs}$  spikes in early April at the PCY station, wherein the  $^{131}\text{I}$  plume arrived earlier than the  $^{137}\text{Cs}$  plume, resulting in surprisingly low  $^{131}\text{I}/^{137}\text{Cs}$  ratios of 0.29 on April 6 and 0.61 on April 7. This  $^{137}\text{Cs}$  plume subsequently arrived at NK in the Taipei Basin, resulting in a trapping effect and, in turn, mixing (coupling) with the  $^{131}\text{I}$  plume to increase the  $^{131}\text{I}/^{137}\text{Cs}$  ratios to around 1. The variability in  $^{131}\text{I}/^{137}\text{Cs}$  ratios might be indicative of either their differential release, with respect to changing degrees of the reactor meltdown, or their differential dispersion. Regardless, its low ratios at nearly 1.0 have never been detected in any wave of radiation clouds that arrived at each mid-latitude site discussed in this study. This may further reveal that both  $^{131}\text{I}$  and  $^{137}\text{Cs}$  in the FRCs would be fractionated during their journey around the globe because of their distinctive characteristics. For instance,  $^{131}\text{I}$  might be more likely to behave like a gaseous pollutant (or submicron aerosol). In contrast,  $^{137}\text{Cs}$  might behave like supermicron aerosol particles.  $^{137}\text{Cs}$ -enriched clouds might be confined within a thinner layer (i.e., the marine and/or planetary boundary), which is supported by our data that presents low  $^{131}\text{I}/^{137}\text{Cs}$  ratios from PCY and NK. In contrast,  $^{131}\text{I}$ -enriched vapours can explode into a

relatively thick layer. This may affect the dispersion rate and the removal of the radioactive particles.

[14] Based on the scenarios described above, a conceptual model is constructed to illustrate the hemispheric transport of  $^{131}\text{I}$  and  $^{137}\text{Cs}$ , as demonstrated in Figure 4. (1) The initial emission from Fukushima had an  $^{131}\text{I}/^{137}\text{Cs}$  ratio of around 2–5, with  $^{131}\text{I}$  residing primarily in the gaseous phase.  $^{131}\text{I}$  may move faster than  $^{137}\text{Cs}$  and readily ascend through convective airs, leading to the separation of  $^{131}\text{I}$ -rich and  $^{137}\text{Cs}$ -rich clouds. (2) Both  $^{131}\text{I}$  and  $^{137}\text{Cs}$  concentrations in the radiation clouds gradually decreased because of dilution by mixing with the ambient air, along with decay and sedimentation. The latter two factors carry different weights in the removal of  $^{131}\text{I}$  and  $^{137}\text{Cs}$ . For the longer-lived  $^{137}\text{Cs}$ , there is little radioactive decay but it is more easily removed by precipitation due to its association with coarser particles [Jost *et al.*, 1986]. (3) Due to its gaseous state initially and association with finer particles later, the residence time of  $^{131}\text{I}$  is longer than that of  $^{137}\text{Cs}$  which is associated with coarser particles. Thus, the  $^{131}\text{I}/^{137}\text{Cs}$  ratio may increase downwind, more than compensating for the decay of  $^{131}\text{I}$ . (4) The absence of the Fukushima-emitted fission products in the TP samples collected before April suggests that the eastward transport through the prevailing westerlies was confined below  $\sim 3\text{--}4$  km for the first wave of radioactive clouds, and their presence in the April 1–6 sample reveals that the clouds extended up to 5 km or higher. (5) When approaching the TP, the first wave of the radioactive air stream (green-tinted in Figure 4) was impeded by the landform, leading to its bifurcation. As for the second wave of radioactive clouds (red-tinted in Figure 4), they may extend to an altitude of  $\sim 5$  km or higher, passing over the TP for further transport.

#### 4. Summary and Implications

[15] Our results offer a valuable archive of data on the Fukushima nuclear accident. Specifically, there is currently

little data on the vertical distribution of radionuclides in the Fukushima disaster. Here, we report the observations at two high mountain stations, covering 3 km to 5 km high. Our observation stations are under the influence of different prevailing wind flows, the lower northeastern monsoon and the upper westerly jet streams. These are useful to identify the different behaviors of  $^{131}\text{I}$  and  $^{137}\text{Cs}$  during dispersion. Worldwide data collected on the radionuclide activities and behaviors emitted by the Fukushima Power Plants, with emphasis on the mid-latitudes, show an exponential-like decrease eastward around the globe for both  $^{131}\text{I}$  and  $^{137}\text{Cs}$ . The journey of these radioactive particles around the globe took  $\sim 18$  days. A conceptual model was constructed to illustrate the hemispheric transport of the initial two waves of radiation plumes. This offers implications for the long-range transport of gaseous and particulate pollutants.

[16] **Acknowledgments.** We thank J. P. Chen for the valuable consultation, and the National Central University for providing the sampling site at Mt. Lulin. This work was supported by grants from the Taiwan NSC (NSC 99-2611-M-001-005, NSC97-2611-M-001-002-MY3, NSC99-2628-M-001-006, NSC 99-2111-M001-007-MY3, NSC 99-2621-M-002-025, and NSC 99-2621-M-002-025) and from the NSF (40875075). The first two authors have equal contribution to the paper.

[17] The Editor thanks two anonymous reviewers for their assistance in evaluating this paper.

## References

- Bluth, G. J. S., S. D. Doiron, C. C. Schnetzler, A. J. Krueger, and L. S. Walter (1992), Global tracking of the  $\text{SO}_2$  clouds from the June, 1991 Mount Pinatubo eruption, *Geophys. Res. Lett.*, *19*, 151–154, doi:10.1029/91GL02792.
- Bowyer, T. W., et al. (2011), Elevated radionuclides detected remotely following the Fukushima nuclear accident, *J. Environ. Radioact.*, *102*, 681–687, doi:10.1016/j.jenvrad.2011.04.009.
- Brandt, J., J. H. Christensen, and L. M. Frohn (2002), Modelling transport and deposition of caesium and iodine from the Chernobyl accident using the DREAM model, *Atmos. Chem. Phys.*, *2*, 397–417, doi:10.5194/acp-2-397-2002.
- Fujii, Y., K. Satake, S. Sakai, M. Shinohara, and T. Kanazawa (2011), Tsunami source of the 2011 off the Pacific coast of Tohoku earthquake, *Earth Planets Space*, *63*, 815–820, doi:10.5047/eps.2011.06.010.
- Harrison, R. M., et al. (1993), Atmospheric pathways, in *Radioecology After Chernobyl: Biogeochemical Pathways of Artificial Radionuclides*, edited by F. S. Warner and R. M. Harrison, pp. 55–100, John Wiley, Chichester, U. K.
- Hsu, S. C., et al. (2010), Effects of acidic processing, transport history, and dust and sea salt loadings on the dissolution of iron from Asian dust, *J. Geophys. Res.*, *115*, D19313, doi:10.1029/2009JD013442.
- Huh, C. A., S. C. Hsu, and C. Y. Lin (2012), Fukushima-derived fission nuclides monitored around Taiwan: Free tropospheric versus boundary layer transport, *Earth Planet. Sci. Lett.*, doi:10.1016/j.epsl.2011.12.004, in press.
- Jost, D. T., H. W. Gäggeler, U. Baltensperger, B. Zinder, and P. Haller (1986), Chernobyl fallout in size-fractionated aerosol, *Nature*, *324*, 22–23, doi:10.1038/324022a0.
- Manolopoulou, M., E. Vagena, S. Syoulos, A. Loannidou, and C. Papastefanou (2011), Radioiodine and radiocesium in Thessaloniki, Greece due to the Fukushima nuclear accident, *J. Environ. Radioact.*, *102*, 796–797, doi:10.1016/j.jenvrad.2011.04.010.
- Masson, O., et al. (2011), Tracking of airborne radionuclides from the damaged Fukushima Dai-Ichi nuclear reactors by European networks, *Environ. Sci. Technol.*, *45*, 7670–7677, doi:10.1021/es2017158.
- Morino, Y., T. Ohara, and M. Nishizawa (2011), Atmospheric behavior, deposition, and budget of radioactive materials from the Fukushima Daiichi nuclear power plant in March 2011, *Geophys. Res. Lett.*, *38*, L00G11, doi:10.1029/2011GL048689.
- Normile, D. (2011), Fukushima revives the low-dose debate, *Science*, *332*, 908–910, doi:10.1126/science.332.6032.908.
- Priyadarshi, A., G. Dominguez, and M. H. Thiemens (2011), Evidence of neutron leakage at the Fukushima nuclear plant from measurements of radioactive  $^{35}\text{S}$  in California, *Proc. Natl. Acad. Sci. U. S. A.*, *108*, 14,422–14,425, doi:10.1073/pnas.1109449108.
- Pudykiewicz, J. (1989), Simulation of the Chernobyl dispersion with a 3-D hemispheric tracer model, *Tellus, Ser. B*, *41*, 391–412, doi:10.1111/j.1600-0889.1989.tb00317.x.
- Stohl, A., P. Seibert, G. Wotawa, D. Arnold, J. F. Burkhart, S. Eckhardt, C. Tapia, A. Vargas, and T. J. Yasunari (2011), Xenon-133 and caesium-137 releases into the atmosphere from the Fukushima Dai-ichi nuclear power plant: Determination of the source term, atmospheric dispersion, and deposition, *Atmos. Chem. Phys. Discuss.*, *11*, 28,319–28,394, doi:10.5194/acpd-11-28319-2011.
- Takemura, T., H. Nakamura, M. Takigawa, H. Kondo, T. Satomura, T. Miyasaka, and T. Nakajima (2011), A numerical simulation of global transport of atmospheric particles emitted from the Fukushima Daiichi Nuclear Power Plant, *Sci. Online Lett. Atmos.*, *7*, 101–104, doi:10.2151/sola.2011-026.
- Tokyo Electric Power Company (2011), Status of cores at units 2 and 3 in Fukushima Daiichi Nuclear Power Station, May 23, 2011, 12 pp., Tokyo.
- Uno, I., et al. (2009), Asian dust transported one full circuit around the globe, *Nat. Geosci.*, *2*, 557–560, doi:10.1038/ngeo583.
- C.-Y. Chan, School of Environmental Science and Engineering, Sun Yat-Sen University, Guangzhou 510275, Guangdong, China.
- S.-C. Hsu, S.-H. Lin, and S. C. Liu, Research Center for Environmental Changes, Academia Sinica, PO Box 1-48, Nankang, Taipei 11529, Taiwan. (schsu815@rccc.sinica.edu.tw)
- C.-A. Huh, Institute of Earth Sciences, Academia Sinica, 128, Sec. 2, Academy Rd., PO Box 1-55, Nankang, Taipei 11529, Taiwan.
- F.-J. Lin, Institute of Oceanography, National Taiwan University, PO Box 23-12, Taipei 11529, Taiwan.